

This is the accepted manuscript made available via CHORUS. The article has been published as:

Dual Nature of Magnetism in a Uranium Heavy-Fermion System

Jooseop Lee, Masaaki Matsuda, John A. Mydosh, Igor Zaliznyak, Alexander I. Kolesnikov, Stefan Süllo, Jacob P. C. Ruff, and Garrett E. Granroth

Phys. Rev. Lett. **121**, 057201 — Published 30 July 2018

DOI: [10.1103/PhysRevLett.121.057201](https://doi.org/10.1103/PhysRevLett.121.057201)

The dual nature of magnetism in a uranium heavy fermion system

Jooseop Lee^{1,2,*}, Masaaki Matsuda³, John A. Mydosh⁴, Igor Zaliznyak⁵, Alexander

I. Kolesnikov³, Stefan Süllow⁶, Jacob P. C. Ruff¹, and Garrett E. Granroth³

¹*CHESS, Cornell University, Ithaca, NY 14853, USA*

²*CALDES, Institute for Basic Science, Pohang 37673, Korea*

³*Neutron Scattering Division, Oak Ridge National Laboratory, Oak Ridge, Tennessee 37831, USA*

⁴*Kamerlingh Onnes Laboratory and Lorentz Institute,
Leiden University, 2300 RA Leiden, The Netherlands*

⁵*CMPMSD, Brookhaven National Laboratory, Upton, New York 11973, USA and*

⁶*Technische Universität Braunschweig, Braunschweig, Germany*

(Dated: July 9, 2018)

The duality between localized and itinerant nature of magnetism in $5f$ electron systems has been a longstanding puzzle. Here, we report inelastic neutron scattering measurements, which reveal both local and itinerant aspects of magnetism in a single crystalline system of UPt_2Si_2 . In the antiferromagnetic state, we observe broad continuum of diffuse magnetic scattering with a resonance-like gap of ≈ 7 meV, and surprising absence of coherent spin-waves, suggestive of itinerant magnetism. While the gap closes above the Neel temperature, strong dynamic spin correlations persist to high temperature. Nevertheless, the size and temperature dependence of the total magnetic spectral weight can be well described by local moment with $J = 4$. Furthermore, polarized neutron measurements reveal that the magnetic fluctuations are mostly transverse, with little or none of the longitudinal component expected for itinerant moments. These results suggest that a dual description of local and itinerant magnetism is required to understand UPt_2Si_2 , and by extension, other $5f$ systems in general.

The degree of localization of magnetic moments is an important concept for understanding many exotic phenomena in condensed matter, thereby creating the “duality” problem [1]. The situation is even more complex in multi-band electronic systems, where the localization can be orbital-selective. For example, the magnetism in iron-based superconductors has been long discussed in terms of either itinerant or local moment only models. Recent progress in this field, however, suggests that this system belong to the intermediate coupling region with $U/W \approx 1$ (U : Coulomb repulsion, W : bandwidth) where we do not have a good understanding yet even for a single band [2].

Ternary intermetallic uranium compounds UT_2M_2 (T : a transition metal, M : Si or Ge) have been of great interest in strongly correlated electron physics during the last decades. URu_2Si_2 has a very small magnetic moment and shows the famous, yet-to-be-understood, phenomena of the hidden order and unconventional superconductivity [3]. UPt_2Si_2 , on the other hand, has been long considered a rare example of uranium intermetallic compound with strongly localized f -electrons. It orders antiferromagnetically ($T_N=32$ K) along c -axis with a magnetic moment of $\approx 2 \mu_B/U$ [4]. Early studies suggested that magnetic anisotropy, high field magnetization, as well as temperature dependence of magnetic susceptibility can be well described within a local-moment crystal electric field (CEF) model [5, 6].

Recent high field studies [7, 8], however, question the degree of localization in this system, suggesting that the observed phase transitions under applied magnetic field can be understood as Lifshitz transitions, an abrupt

change in the topology of a Fermi surface. This view is further supported by the density functional theory (DFT) [9], which indicates that $5f$ electrons in UPt_2Si_2 system are orbitally polarized and mostly itinerant, with only a slight tendency toward localization.

In order to understand the magnetism, specifically the interplay between local and itinerant nature of the moments in this system, it is crucial to study the spin dynamics. However, magnetic excitations in UPt_2Si_2 have not been observed, despite the large ordered magnetic moment. An early inelastic neutron scattering study [10] provided very limited information (at 77 K) due to the polycrystalline nature of the sample, while a more recent work [11] did not find any spin waves below ~ 3 meV.

Here, we present comprehensive neutron inelastic scattering results demonstrating that both itinerant and local moments nature of f -electrons are playing a role in this system. We observe a diffuse magnetic excitation continuum with a resonance-like gap of ≈ 7 meV, which clearly cannot be explained by spin wave theory for coherent collective excitation of localized moments. Rather, the excitation can be understood within the random-phase approximation (RPA) model response of the itinerant system. The size and temperature dependence of the total magnetic moment, however, can be well described by local model with $J = 4$, a total angular momentum associated with a local magnetic moment, $\hat{\mu} = g\mu_B\hat{J}$. Polarized neutron measurements also reveal that the fluctuations are mostly transverse to the staggered ordered moment. While an ordered local moment produces a transverse fluctuation, an itinerant moment also has longitudinal dynamics corresponding to the fluctuation of

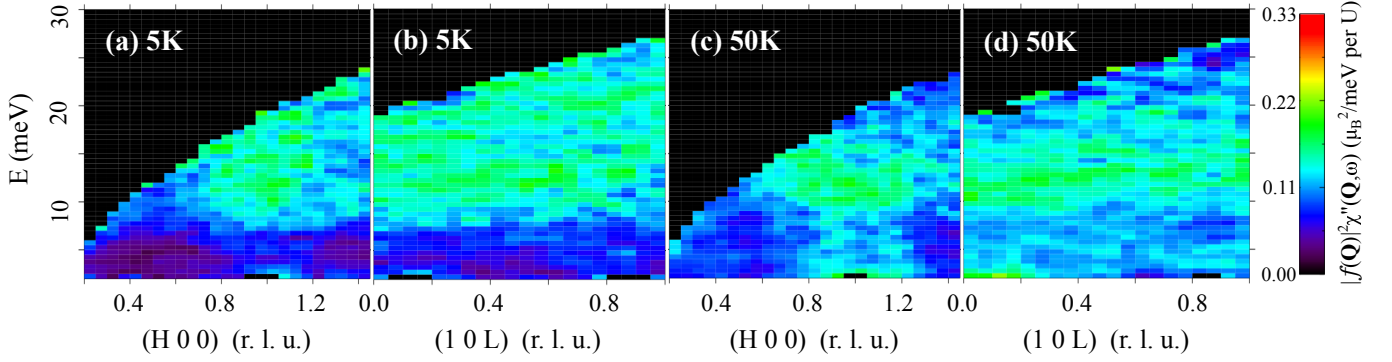


FIG. 1. The imaginary part of the dynamical magnetic susceptibility, $\chi''(\mathbf{Q}, \omega)$, corrected for U^{4+} magnetic form factor, at 5 K ((a) and (b)) and 50 K ((c) and (d)). The measurement was performed at SEQUOIA, with incident energy $E_i = 50$ meV.

the size of the magnetic moment [1]. These observations show that even in this large magnetic moment system a dual approach based on itinerant and local description is necessary to fully capture its nature. The duality of magnetism was also suggested in other heavy fermion superconductors [12], and thus seems to be universal across $5f$ electron systems.

All measurements presented here were performed on a 1.5 g single crystalline sample of $U\text{Pt}_2\text{Si}_2$ [13]. Initial neutron scattering measurements were done with the HB1 thermal triple axis spectrometer (TAS) at the HFIR, ORNL. A large volume of energy-momentum space was then explored using the time-of-flight (TOF) spectrometer SEQUOIA [16, 17] at SNS, ORNL [18] with incident energies (E_i) of 50 meV and 100 meV. TOF neutron data was normalized to the absolute scattering cross-section in $\mu_B^2/\text{meV}/U$ by using a standard vanadium sample [19]. The measured scattering intensities were converted to the imaginary part of the dynamical magnetic susceptibility via the fluctuation-dissipation theorem, $\chi''(\mathbf{Q}, \omega) = \pi(1 - e^{-E/k_B T})S(\mathbf{Q}, \omega)$ [20].

Contrary to what is expected for conventional magnetic order, a broad continuum of magnetic excitations is observed around the magnetic wave vector, $\mathbf{Q}_M = (1\ 0\ 0)$, Fig. 1. In the local magnetism approach, interactions between local moments are described by a spin exchange Hamiltonian. The low-energy collective transverse fluctuations of ordered magnetic moments, i.e., spin waves are expected to have well-defined sharp dispersion relations demonstrating long-range coherence. In an itinerant moment system, on the other hand, the excitations originate from electron-hole pairs created across the Fermi surface. These excitations are usually broad in \mathbf{Q} - E space and weak in intensity, without clear dispersion.

Figure 1 (a,b) presents the generalized susceptibility as a function of wave vector along $(H\ 0\ 0)$ and $(1\ 0\ L)$ direction, respectively, at $T \ll T_N$. The excitation is diffuse, centered around $E \approx 13$ meV, with a gap ≈ 7 meV. The intensity in H -direction is peaked near \mathbf{Q}_M . The

excitation along L -direction (Fig. 1 (b)), in contrast, is rather flat, suggesting anisotropic magnetic interactions consistent with the quasi two-dimensional (2D) character observed in resistivity [21] and Fermi surface [9]. A spin gap of ~ 7 meV, which is clearly visible in Fig. 1 (a,b) is roughly consistent with the gap of 46 K estimated from the temperature dependence of resistivity [21]. Above the Neel temperature, at 50 K, this gap is closed, as shown in Fig. 1 (c,d). It should be noted that spin fluctuations along $(H\ 0\ 0)$ are still clearly peaked around \mathbf{Q}_M , indicating strong magnetic correlation even in the paramagnetic regime above T_N . We refer to the supplementary material for more temperature dependence data [22].

As the observed excitation continuum cannot be described by spin wave theory, we fit the data using the dynamical magnetic susceptibility calculated using Random Phase Approximation (RPA) in an itinerant electron model. The resulting expression is essentially identical to the extended Self-Consistent Renormalization (SCR) theory model [1, 23, 24], which takes account, in a self-consistent way, of the effect of the spin fluctuation mode coupling [25]. The resulting RPA-SCR expression for the generalized magnetic susceptibility is,

$$\chi''(\mathbf{Q}+\mathbf{q}, \omega) = \frac{\chi_Q}{1 + (q/\kappa)^2} \frac{\hbar\omega\Gamma(q, \kappa)}{(\hbar\omega)^2 + \Gamma(q, \kappa)^2}, \quad (1)$$

with the \mathbf{Q} -dependent relaxation rate,

$$\Gamma(q, \kappa) = \gamma_A (\kappa^2 + q^2). \quad (2)$$

Parameters κ , γ_A , and χ_Q are a characteristic width in reciprocal space, a temperature-insensitive energy width parameter, and a static staggered susceptibility, respectively. The wave vector q is measured away from \mathbf{Q}_M .

It is clear from Fig. 2 that Eq. 1 provides adequate description of the observed magnetic excitation. While data with $E_i = 50$ meV reveals the 7 meV gap with better resolution, $E_i = 100$ meV data capture the full range of magnetic excitation and, therefore, was used

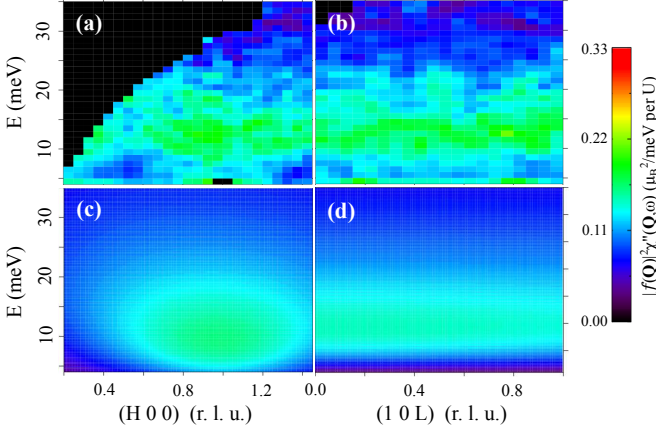


FIG. 2. (a) and (b) $\chi''(\mathbf{Q}, \omega)$ observed at 50K with $E_i = 100$ meV along H and L direction, respectively. (c) and (d) Fit to SCR, or equivalently, RPA theoretical model.

for the global fitting. The results of the fit along the H and L directions are shown in Fig. 2 (c,d). Table I lists the best fit parameters when magnetic form factor is co-refined [26, 27]. The top of the excitation band is around 25 meV. The single intensity lobe is inconsistent with dispersive magnetic excitations. This demonstrates that the spin fluctuation is rather a resonance localized in Q-E space, similar to the resonance magnetic excitation observed in many unconventional superconductors such as cuprates [31], Fe-based superconductors [2], or heavy fermion superconductors [32].

Figure 3 shows the change in scattering intensity with varying temperature. There is an increase of quasi-elastic paramagnetic scattering with the increasing temperature across T_N . The change of the spectral gap follows the order parameter dependence of magnetic Bragg peaks [4], which strongly supports the magnetic nature of fluctuations [33].

The spectral weight filling in the gap comes from other energy transfers, Fig. 3 (b). It is clear, however, from Figs. 1 and 3, that this redistribution affects only a moderately small fraction of the total magnetic spectral weight. In this case, the ordered magnetic moment in the antiferromagnetic state, which is only $2 \mu_B$, is weak and comprises only a small fraction of the fluctuating magnetic moment. Consequently, its influence on magnetic excitations is small and limited to low energies, $\lesssim k_B T_N$, which again emphasizes that the system cannot be simply understood from its ordered moment [34].

	$\kappa [\text{\AA}^{-1}]$	$\gamma_A [\text{meV}/\text{\AA}^{-2}]$	$\chi_Q [\mu_B^2/\text{meV}]$
(H 0 0)	1.35(8)	5.18(54)	0.33(1)
(1 0 L)	2.77(114)	1.21(98)	0.30(1)

TABLE I. Parameters obtained by fitting $E_i=100$ meV and $T=50$ K data with Eq. 1.

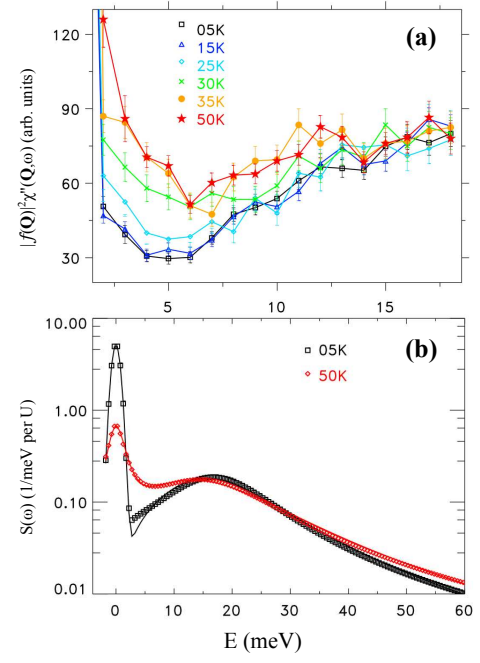


FIG. 3. Evolution of the generalized susceptibility across T_N . (a) The detailed temperature dependence of low energy spin excitation at $Q=(1\ 0\ 0)$ measured using HB1 triple axis spectrometer. Counting time for each data point was about 5 minutes. (b) The autocorrelation function, $S(E)$, at 5 K (black square) and 50K (red diamond), obtained from Q-integrated spectral weight of the TOF data. Solid lines show fit to a model function consisting of a Lorentzian centered at $E = 0$ (quasi-elastic) and a damped harmonic oscillator (inelastic).

In the local moment model, the integral spectral weight measured by neutron scattering obeys the zero-moment sum rule [20], $\sum_{\alpha} \int_{-\infty}^{+\infty} \int_{BZ} S^{\alpha\alpha}(\mathbf{q}, \omega) d\mathbf{q} d\omega / \int_{BZ} d\mathbf{q} = (g\mu_B)^2 J(J+1)$, where α is the polarization of magnetic fluctuation, g is the spectroscopic Lande g-factor, μ_B is Bohr magneton. By assuming random polarization of magnetic fluctuation with respect to the wave vector transfer, which is a good approximation for the TOF data in Fig. 3 (b), and fitting the Q-integrated normalized magnetic intensity [35], $S(E)$, to a model function consisting of the quasielastic Lorentzian and the damped harmonic oscillator (DHO), we obtain the integral magnetic scattering intensity of $\approx 15.9\mu_B^2$ at 5 K and $\approx 13.6\mu_B^2$ at 50 K. Using $g = 0.8$, which is appropriate for the 3H_4 Hund rule Russell-Saunders ground state of U^{4+} [36], this results in estimated $J \approx 4.5$ at 5 K and ≈ 4.1 at 50 K, consistent with the $J = 4$ state. This exhausts the full magnetic spectral weight available for the $5f^2$ electronic configuration of U^{4+} and, therefore, temperature enhancement of integral spectral weight from the entanglement between local and itinerant electrons [37] is not observed.

The integral intensity of the magnetic excitation spectrum thus indicates participation of two $5f$ electrons, as

in the $J = 4$ state of U^{4+} in the local-moment picture. In order to rationalize the observed magnetic spectral weight in the itinerant-electron model of Eq. 1, one needs to recall that the approximation adopted in deriving this result [1, 23, 24] limits its applicability to the proximity of the Fermi energy. Hence, the integration of the spectral weight must be limited by a finite-energy cut-off, Λ , which is of the order of the itinerant-electron bandwidth (otherwise the integral formally diverges). On account of this cutoff, the total magnetic spectral weight is, $\int_{-\infty}^{+\infty} \int_{BZ} \chi''(\mathbf{q}, \omega) d\mathbf{q} dE / \int_{BZ} d\mathbf{q} \approx \chi_Q(\gamma_A \kappa^2) \ln \left(\frac{\Lambda}{\gamma_A \kappa^2} \right)$ [38]. Using the fit results from Table I we estimate the itinerant-electron bandwidth of $1 \sim 2$ eV, in good agreement with the extent of spin-polarized $5f$ bands in recent DFT calculations [8, 9]. Hence, UPt_2Si_2 cannot be simply viewed as narrow-band system where local-moment picture applies. The observed magnetic dynamics inside the energy window probed in the present experiment is distinct from that of local moments and is well described by the RPA itinerant-electron theory. On the other hand, applying the first moment sum rule to the measured intensity and assuming local moment model with nearest neighbor exchange interactions we obtain a much lower energy scale, ≈ 10 meV, for the contribution of magnetic bond energies per U to the ground state, consistent with the observed excitation spectrum [39].

In order to further elucidate the magnetic nature of the observed diffuse and weak excitation, we carried out a polarized neutron measurement. Table II summarizes different contributions to the spin-flip (SF) and non-spin-flip (NSF) intensities when the scattering plane is (H 0 L) and the neutron spin is parallel to either a -axis (HF: horizontal field) or b -axis (VF: vertical field) directions. Since U magnetic moments are aligned along c -axis, $S_{a,b}$ corresponds to transverse fluctuations while S_c indicates a longitudinal fluctuation.

Figure 4 presents polarized neutron scans below T_N at constant $E=12$ meV along (H 0 0) direction, which reveal small but clear magnetic signal whose Q -dependence is consistent with that observed with unpolarized neutrons (Fig. 2). The polarization of magnetic fluctuation can be further analyzed by comparing different scattering setups. The intensity difference between HF and VF

	HF ($\mathbf{P}_n \parallel a$)	VF ($\mathbf{P}_n \parallel b$)
SF	$S_b^2 + S_c^2 + B_1$	$S_c^2 + B_1$
NSF	$N^2 + B_2$	$S_b^2 + N^2 + B_2$

TABLE II. Nuclear and magnetic components contributing to the scattering intensity at (H 0 0) in the present polarized neutron measurement. P_n is the neutron spin polarization direction, N denotes nuclear components, and $B_{1,2}$ represent background in SF and NSF configuration, respectively. S_a cannot be observed in this setup because magnetic component parallel to \mathbf{Q} does not contribute to neutron scattering.

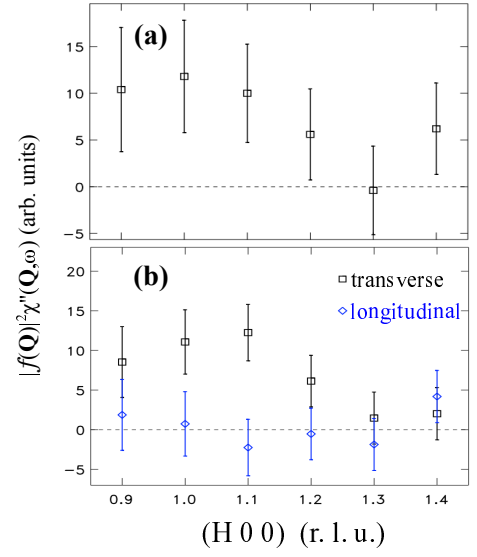


FIG. 4. Polarized neutron measurement at constant $E=12$ meV at $T=5$ K. (a) Magnetic scattering (= HF-SF – HF-NSF in Table II). (b) Transverse spin fluctuation, S_b (=HF-SF – VF-SF or VF-NSF – HF-NSF), and estimated longitudinal spin fluctuation, S_c (=HF-SF – VF-NSF or VF-SF – HF-NSF). Each data point has been counted for about 3 hours.

configuration, either in SF or NSF, directly yields S_b , the transverse fluctuation. Black squares in Fig. 4 (b) show the transverse fluctuation. The longitudinal component can be evaluated from the difference of HF-SF and VF-NSF (or VF-SF and HF-NSF) assuming that $N^2 + B_2$ and B_1 do not differ, which is valid since the total magnetic signal (Fig. 4 (a)) correspond to the sum of transverse and longitudinal signals (Fig. 4 (b)). The estimated longitudinal fluctuation shown as blue diamond symbols in Fig. 4 (b) appears to have negligible intensity. This indicates that spin fluctuations are primarily transverse, in sharp contrast with the longitudinal magnetic dynamics observed in chromium, the archetypal example of an itinerant antiferromagnet [41] and in other uranium compounds such as UN [42] and URu_2Si_2 [43].

Our comprehensive inelastic neutron scattering studies thus show that itinerant electrons are playing a major role in the dynamical magnetism of UPt_2Si_2 . Despite the large ordered magnetic moment revealed by neutron diffraction [4], the magnetic excitations are broad and resonance-like, lacking a sharp dispersion, and could be understood in itinerant RPA approach. Above T_N , the gap in the excitation spectrum is closed, but the strong magnetic correlation is still present. The temperature dependence of spectral weight shows that only small fraction of magnetic excitation changes across the Neel temperature and the system should not be described solely from its ordered moment.

Our results make it clear that this system is at the boundary where both local moment and itinerant degrees of freedom are important, just like Fe-based superconductors or other strongly correlated electron systems. Many physical properties previously attributed exclusively to local nature, for example, field induced phase transitions [7] could be indeed consequences of this magnetic duality. Lack of adequate theory to comprehensively describe the observed behaviors call for new modeling effort with UPt_2Si_2 as a test case for duality. Considering the universal magnetic duality in $5f$ -electron systems, other overlooked large moment uranium intermetallics [44–47] should be also re-examined.

ACKNOWLEDGMENT

We thank Guangyong Xu and T. J. Williams for helpful discussion on data analysis. This research at High Flux Isotope Reactor and Spallation Neutron Source of ORNL was sponsored by the Scientific User Facilities Division, Office of Basic Energy Sciences, U.S. Department of Energy and the Laboratory Directors Research and Development fund of ORNL. Cornell High Energy Synchrotron Source was supported by the NSF and NIH/National Institute of General Medical Sciences via NSF award no. DMR-1332208. The work at Brookhaven National Laboratory was supported by the Office of Basic Energy Sciences, U.S. Department of Energy, under Contract No. DE-SC0012704.

* Formerly with Quantum Condensed Matter Division, ORNL.

- [1] T. Moriya, *Spin Fluctuations in Itinerant Electron Magnetism*, (Springer-Verlag, Berlin, 1985).
- [2] P. Dai, J. Hu, and E. Dagotto, *Nat. Phys.*, **8**, 709 (2012).
- [3] J. A. Mydosh and P. M. Oppeneer, *Rev. Mod. Phys.*, **83**, 1301 (2011) and the references therein.
- [4] R. A. Steeman, E. Frikkee, S. A. M. Mentink, A. A. Menovsky, G. J. Nieuwenhuys, and J. A. Mydosh, *J. Phys. Condens. Matter*, **2**, 4059 (1990).
- [5] G. J. Nieuwenhuys, *Phys. Rev. B*, **35**, 5260 (1987).
- [6] H. Amitsuka, T. Sakakibara, K. Sugiyama, T. Ikeda, Y. Miyako, M. Date, and A. Yamagishi, *Physica B*, **177**, 173 (1992).
- [7] D. Schulze Grachtrup, M. Bleckmann, B. Willenberg, S. Süllow, M. Bartkowiak, Y. Skourski, H. Rakoto, I. Sheikin, and J. A. Mydosh, *Phys. Rev. B*, **85**, 054410 (2012).
- [8] D. Schulze Grachtrup, N. Steinki, S. Süllow, Z. Cakir, G. Zwirgagl, Y. Krupko, I. Sheikin, M. Jaime, and J. A. Mydosh, *Phys. Rev. B*, **95**, 134422 (2017).
- [9] S. Elgazzar, J. Rusz, P. M. Oppeneer, and J. A. Mydosh, *Phys. Rev. B*, **86**, 075104 (2012).
- [10] R. A. Steeman, E. Frikkee, C. van Dijk, G. J. Nieuwenhuys, and A. A. Menovsky, *J. Magn. Magn. Mater.*, **76**, 435 (1988).
- [11] N. Metoki, Y. Koike, Y. Haga, N. Bernhoeft, G. H. Lander, Y. Tokiwa, and Y. Ōnuki, *Acta Phys. Pol., B*, **34**, 979 (2003).
- [12] S. Fujimori, Y. Saitoh, T. Okane, A. Fujimori, H. Yamagami, Y. Haga, E. Yamamoto, and Y. Ōnuki, *Nat. Phys.*, **3**, 618 (2007).
- [13] See Supplemental Material for more details on the experimental setup, which includes Ref. [14–15].
- [14] O. Arnold, J. C. Bilheux, J. M. Borreguero, A. Buts, S. I. Campbell, L. Chapon, M. Doucet, N. Draper, R. Ferraz Leal, M. A. Gigg, V. E. Lynch, A. Markvardsen, D. J. Mikkelsen, R. L. Mikkelsen, R. Miller, K. Palmen, P. Parker, G. Passos, T. G. Perring, P. F. Peterson, S. Ren, M. A. Reuter, A. T. Savici, J. W. Taylor, R. J. Taylor, R. Tolchenov, W. Zhou and J. Zikovsky, *Nucl. Instr. Meth. A*, **764**, 156 (2014).
- [15] R. A. Ewings, A. Buts, M. D. Le, J. van Duijn, I. Bustinduy, and T.G. Perring, *Nucl. Instr. Meth. A*, **834**, 132 (2016).
- [16] G. E. Granroth, D. H. Vandergriff, and S. E. Nagler, *Physica B*, **385–86**, 1104 (2006).
- [17] G. E. Granroth, A. I. Kolesnikov, T. E. Sherline, J. P. Clancy, K. A. Ross, J. P. C. Ruff, B. D. Gaulin, and S. E. Nagler, *J. Phys. Conf. Ser.*, **251**, 012058 (2010).
- [18] T. E. Mason, D. Abernathy, I. Anderson, J. Ankner, T. Egami, G. Ehlers, A. Ekkebus, G. Granroth, M. Hagen, K. Herwig, J. Hodges, C. Hoffmann, C. Horak, L. Horton, F. Klose, J. Larese, A. Mesecar, D. Myles, J. Neufeld, M. Ohl, C. Tulk, X-L. Wang, and J. Zhao, *Physica B: Cond. Matt.*, **385**, 955 (2006).
- [19] G. Xu, Z. Xu, and J. M. Tranquada, *Rev. Sci. Instrum.*, **84**, 083906 (2013).
- [20] I. A. Zaliznyak and S.-H. Lee, *Modern Techniques for Characterizing Magnetic Materials*, edited by Y. Zhu (Springer, Heidelberg, 2005).
- [21] S. Süllow, A. Otop, A. Loose, J. Klenke, O. Prokhnenko, R. Feyerherm, R. W. A. Hendrikx, J. A. Mydosh, and H. Amitsuka, *J. Phys. Soc. Jpn.*, **77**, 024708 (2008).
- [22] See Supplemental Material for wider range temperature dependence at different wavevectors.
- [23] H. Hasegawa and T. Moriya, *J. Phys. Soc. Jpn.*, **36**, 1542 (1974).
- [24] K. Nakayama and T. Moriya, *J. Phys. Soc. Jpn.*, **56**, 2918 (1987).
- [25] W. Bao, C. Broholm, G. Aeppli, S. A. Carter, P. Dai, T. F. Rosenbaum, J. M. Honig, P. Metcalf, and S. F. Trevino, *Phys. Rev. B*, **58**, 12727 (1998).
- [26] The error bar does not include systemic errors from absolute normalization, which is typically about 20 %.
- [27] See Supplemental Material for more details on phenomenological magnetic form factor and its refinement, which includes Ref. [28–30].
- [28] Igor Zaliznyak, Andrei T. Savici, Mark Lumsden, Alexei Tselik, Rongwei Hu, and Cedimir Petrovic, *Proc. Nat. Acad. Sci.* **112**, 10316 (2015).
- [29] T. Moriya and K. Ueda, *J. Phys. Soc. Jpn.*, **63**, 1871 (1994).
- [30] W. Knafo, S. Raymond, P. Lejay, and J. Flouquet, *Nat. Phys.*, **5**, 753 (2009).
- [31] J. M. Tranquada, G. Xu, and I. A. Zaliznyak, *J. Magn. Magn. Mater.*, **350**, 148 (2014).

- [32] C. Stock, C. Broholm, J. Hudis, H. J. Kang, and C. Petrovic, Phys. Rev. Lett. **100**, 087001 (2008).
- [33] E. G. Sergeicheva, S. S. Sosin, L. A. Prozorova, G. D. Gu, and I. A. Zaliznyak, Phys. Rev. B, **95**, 020411(R) (2017).
- [34] See Supplemental Material for the SCR-RPA analysis in the AFM phase.
- [35] Since the accessible energy range around $Q=(1\ 0\ 0)$ is limited due to kinematic restriction, we divided BZ into small areas whose integrated intensity is extrapolated to high energy transfer by fitting to Lorentzian distribution. Final integrated intensity in Fig. 3(b) was estimated by summing each integrated intensity weighted by their BZ volume. $E_i=50\text{meV}$ and 100meV data have been used for low ($\leq 10\text{meV}$) and high energy ($\geq 10\text{meV}$) transfer, respectively, which were joined smoothly after absolute normalization.
- [36] A. J. Freeman, J. P. Desclaux, G. H. Lander, and J. Faber, Jr., Phys. Rev. B, **13**, 1168 (1976).
- [37] I. A. Zaliznyak, Z. Xu, J. M. Tranquada, G. Gu, A. M. Tsvelik, and M. B. Stone, Phys. Rev. Lett. **107**, 216403 (2011).
- [38] See Supplemental Material for the estimation of bandwidth in the itinerant-electron system.
- [39] See Supplemental Material for the bond energy from first moment sum rule in neutron scattering, which includes Ref. [40].
- [40] M. B. Stone, I. Zaliznyak, Daniel H. Reich, and C. Broholm, Phys. Rev. B, **64**, 144405 (2001)
- [41] E. Fawcett, Rev. Mod. Phys., **60**, 209 (1988).
- [42] T. M. Holden, W. J. L. Buyers, E. C. Svensson, and G. H. Lander, Phys. Rev. B, **30**, 114 (1984).
- [43] F. Bourdarot, E. Ressouchea, R. Balloub, S. Raymonda, D. Aokia, N. Martina, L.-P. Regnaulta, V. Simonetb, M.T. Fernandez-Diazc, A. Stunaultc, V. Taufoura, and J. Flouquet, Phys. Procedia, **42**, 4 (2013).
- [44] H. Ptasiwicz-Bak, J. Leciejewicz, and A. Zygmunt, J. Phys. F: Metal Phys., **11**, 1225 (1981).
- [45] B. Shemirani, H. Lin, M. F. Collins, C. V. Stager, J. D. Garrett, and W. J. L. Buyers, Phys. Rev. B, **47**, 8672 (1993).
- [46] L. Chelmsicki, J. Leciejewicz, and A. Zygmunt, Solid State Commun., **48**, 177 (1983).
- [47] J. Leciejewicz, L. Chelmsicki, and A. Zygmunt, Solid State Commun., **41**, 167 (1982).